# Supporting Information

**Caption of Figures:**

**Fig. S1.** Formation energies of $Li_xMn_2O_4$ with Li occupying 2a, 2b, 4e, 8h and 8h' sites show the stability following 8h>8h'>4e>2a>2b.
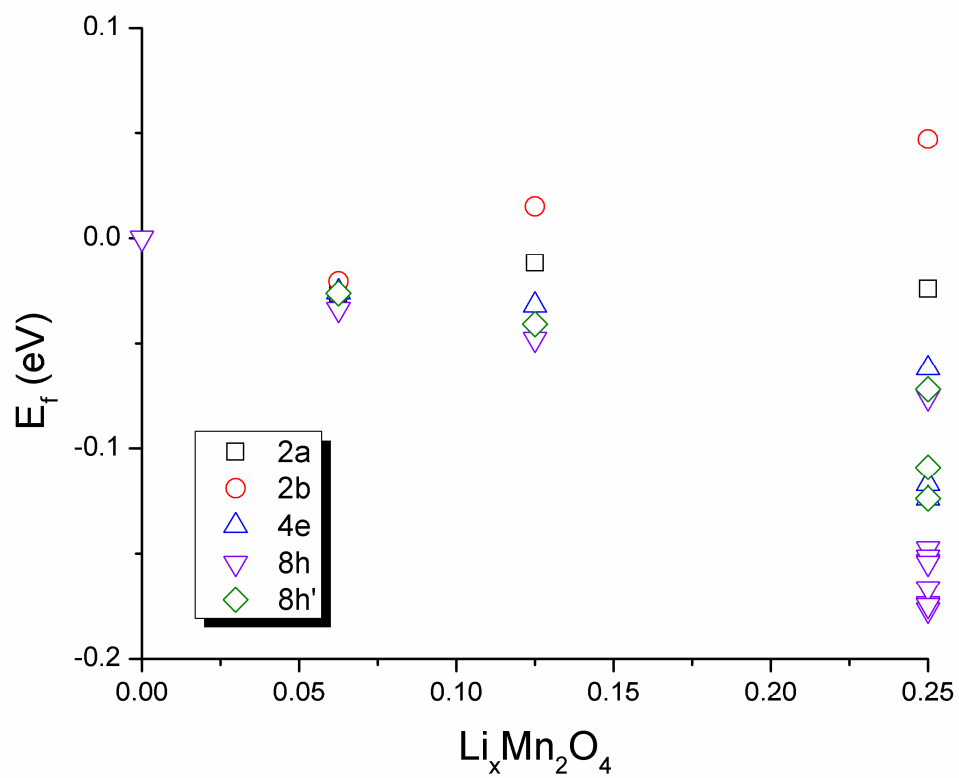
**Fig. S2.** Lattice constant $c$ of $Li_xMn_2O_4$.

**Fig. S3.** Evolution of $\gamma$ for $Li_xMn_2O_4$. The largest deviation between $\gamma$ and 90 □ is 1.0 □, suggesting the structure remains at near-orthorhombic symmetry. For simplicity we regard the symmetry as "orthorhombic" in the manuscript.

**Fig. S4.** Relative energy difference between $Li_{2x}MnO_{2+x}$ configurations with Li(O) occupying 8h(2a) and the most stable configurations in which Li(O) occupies 8h'(2b) sites.

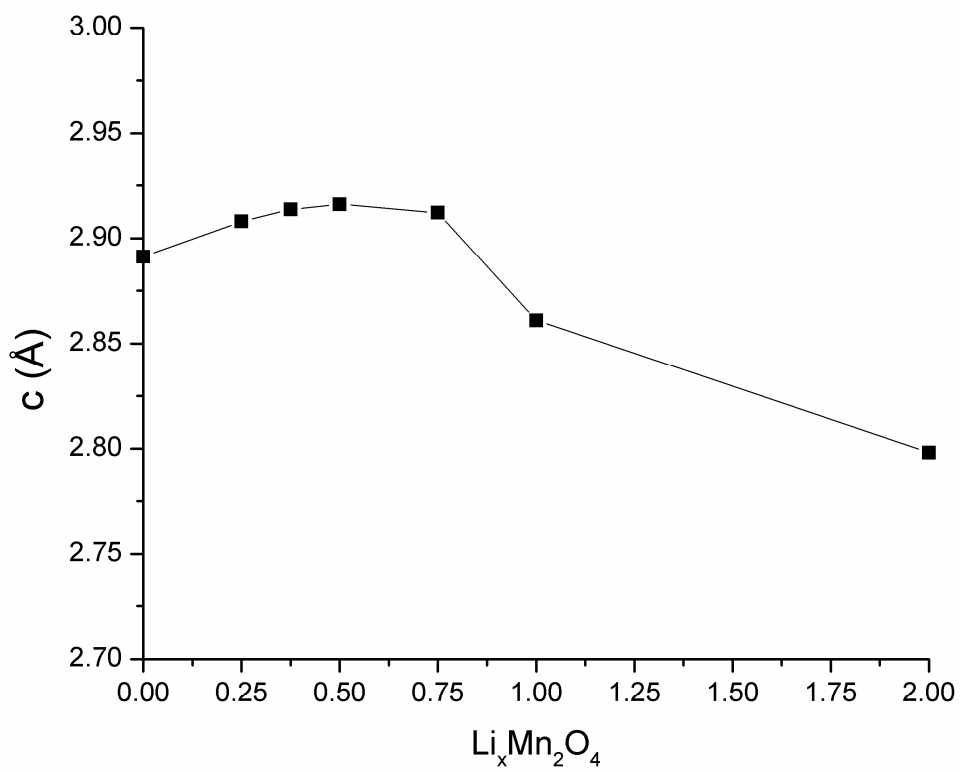**Fig. S5.** Partial Density of States for (a) pristine $MnO_2$ and (b) $0.25Li_2O \cdot MnO_2$. Blue: Mn, Red: framework O, Green: inserted O. For pristine $MnO_2$, the valence band edge is mainly composed of occupied Mn 3d orbitals, while the conduction band edge is composed of both unoccupied Mn 3d and O 2p orbitals. For $0.25Li_2O \cdot MnO_2$ the occupied band near Fermi energy is mainly composed of Mn 3d and framework O 2p orbitals, with minor contribution from inserted O 2p orbitals.

**Fig. S6.** Density of States for (a) pristine $MnO_2$ and (b) $0.25Li_2O \cdot MnO_2$. For pristine $MnO_2$, the valence band edge is mainly composed of occupied Mn 3d orbitals, while the conduction band edge is composed of both unoccupied Mn 3d and O 2p orbitals. For $0.25Li_2O \cdot MnO_2$ the occupied band near Fermi energy is mainly composed of Mn 3d and framework O 2p orbitals, with minor contribution from inserted O 2p orbitals.
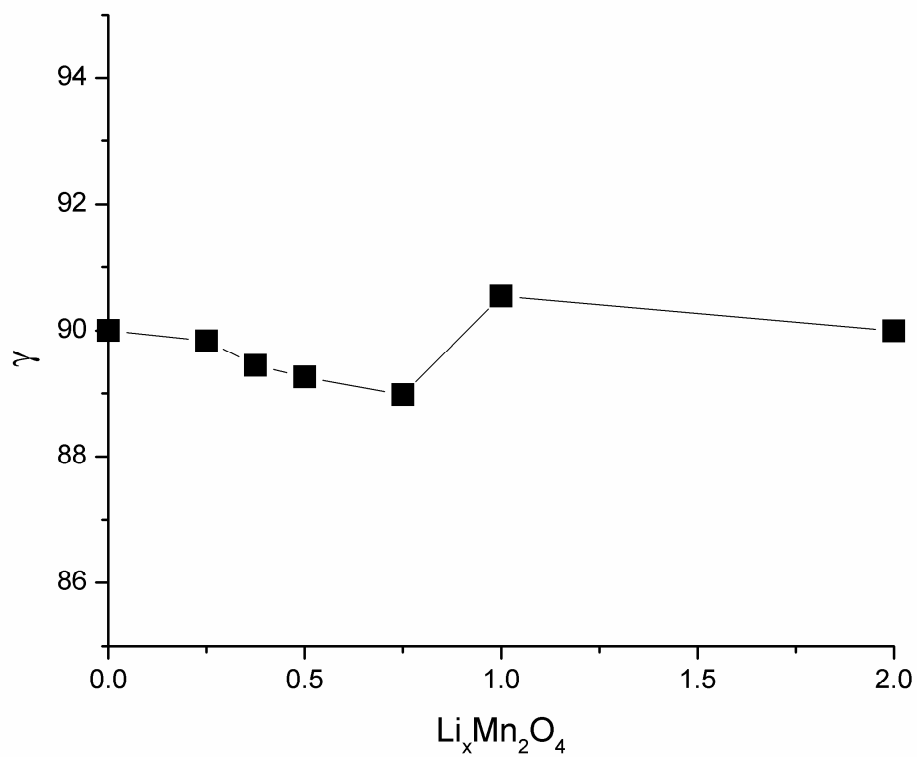
**Fig. S7.** Decomposed Density of States projected on d-orbitals of Mn ions in $LiMn_2O_4$

**Fig. S1.** Formation energies of $Li_xMn_2O_4$ with Li occupying 2a, 2b, 4e, 8h and 8h' sites show the stability following 8h>8h'>4e>2a>2b.

**Fig. S2.** Lattice constant $c$ of $Li_xMn_2O_4$.

**Fig. S3.** Evolution of $\gamma$ for $Li_xMn_2O_4$. The largest deviation between $\gamma$ and 90 □ is 1.0 □, suggesting the structure remains at near-orthorhombic symmetry. For simplicity we regard the symmetry as "orthorhombic" in the manuscript.
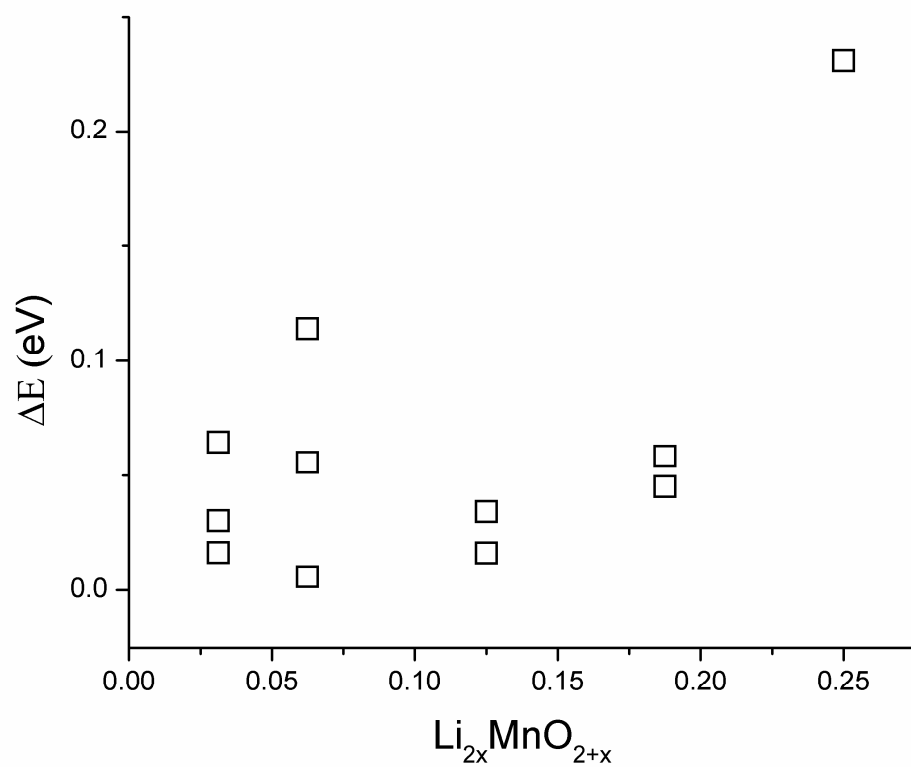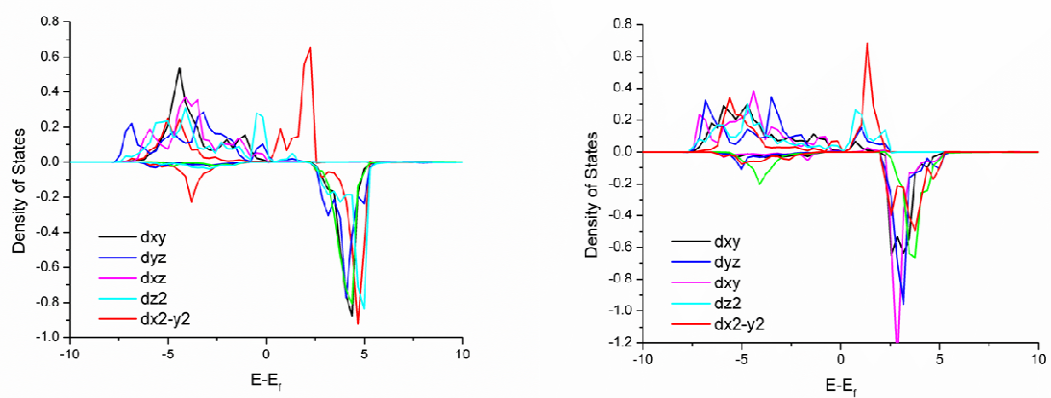
**Fig. S4.** Relative energy difference between $Li_{2x}MnO_{2+x}$ configurations with Li(O) occupying 8h(2a) and the most stable configurations with Li(O) occupying 8h'(2b) sites.
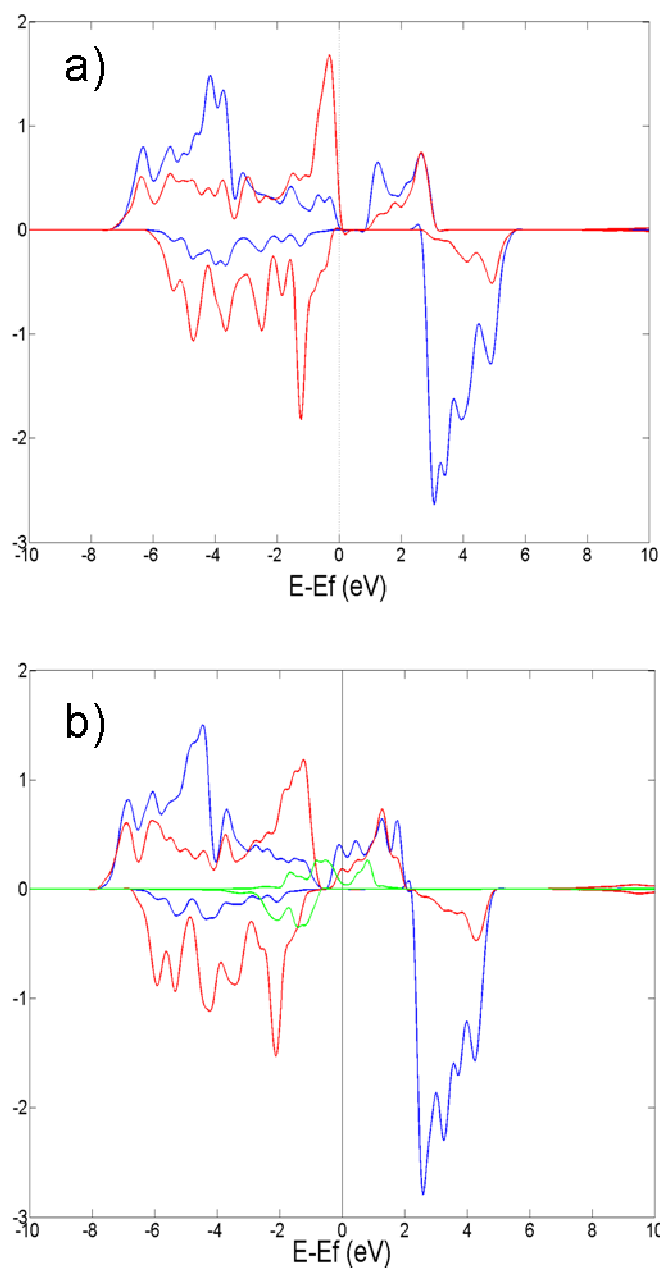
**Fig. S5.** Partial Density of States for (a) pristine $MnO_2$ and (b) $0.25Li_2O \cdot MnO_2$. Blue: Mn, Red: framework O, Green: inserted O. For pristine $MnO_2$, the valence band edge is mainly composed of occupied Mn 3d orbitals, while the conduction band edge is composed of both unoccupied Mn 3d and O 2p orbitals. For $0.25Li_2O \cdot MnO_2$ the occupied band near Fermi energy is mainly composed of Mn 3d and framework O 2p orbitals, with minor contribution from inserted O 2p orbitals.
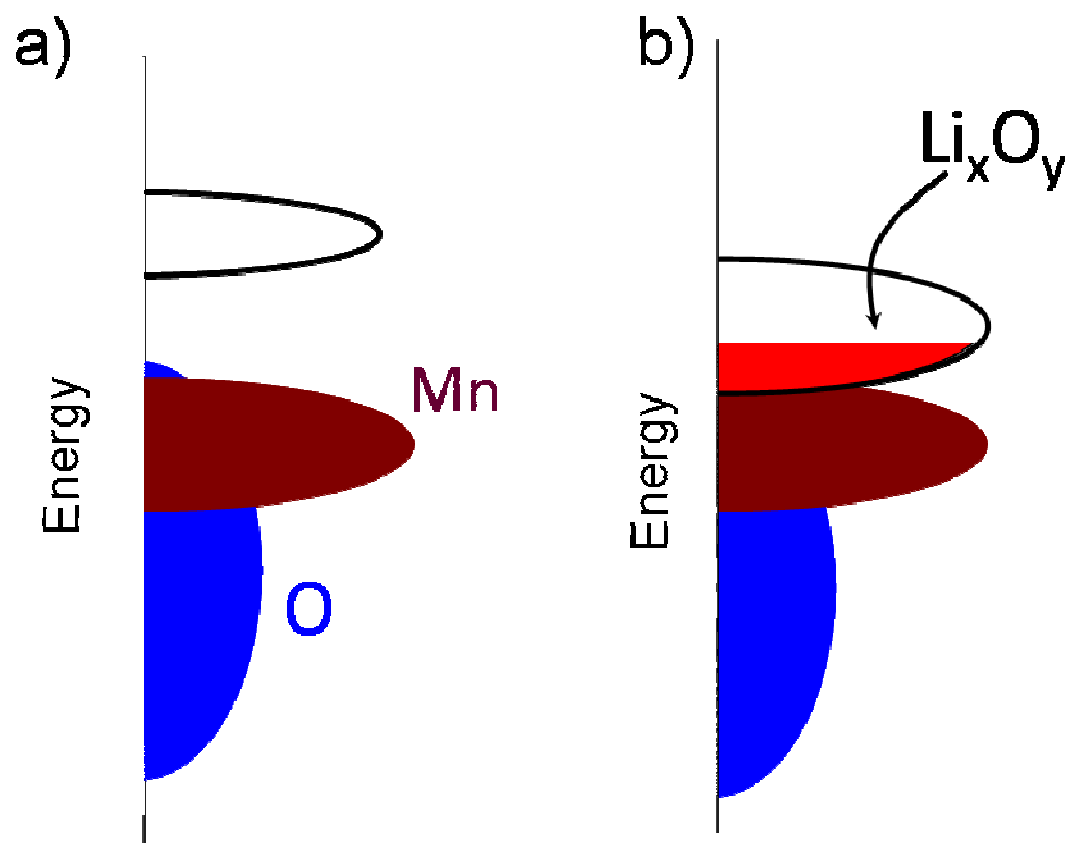
**Fig. S6.** Schematic of the change of the band structure from (a) pristine $\alpha MnO_2$ to (b) $Li_xO_y$ inserted $\alpha MnO_2$.

**Fig. S7.** Decomposed Density of States projected on d-orbitals of Mn ions in LiMn$_2$O$_4$